Elucidation of the secoiridoid pathway in Catharanthus roseus

Miettinen, K.

Chapter 2

Characterization of the plastidial geraniol synthase from Madagascar periwinkle which initiates the monoterpenoid branch of the alkaloid pathway in internal phloem associated parenchyma

Phytochemistry (2013) 85:36-43

Andrew J. Simkin[a,1,†], **Karel Miettinen**[b,†], Patricia Claudel[c], Vincent Burlat[d,e], Grégory Guirimand[a], Vincent Courdavault[a], Nicolas Papon[a], Sophie Meyer[c], Stéphanie Godet[a,2], Benoit St-Pierre[a], Nathalie Giglioli-Guivarc'h[a], Marc J.C. Fischer[c], Johan Memelink[b], Marc Clastre[a,*]

† These authors contributed equally to this work.

[(a)] Université François-Rabelais, EA2106, Biomolécules et Biotechnologies Végétales, 31 avenue Monge, 37200 Tours, France

[(b)] Institute of Biology, Sylvius Laboratory, Sylviusweg 72, PO Box 9505, 2300 RA Leiden, The Netherlands

[(c)] Université de Strasbourg, INRA, Métabolisme secondaire de la vigne, Unité mixte de Recherche Santé Vigne et Qualité des vins, 28 rue de Herrlisheim, 68021 Colmar, France

[(d)] Université de Toulouse, UPS, UMR5546, Laboratoire de Recherche en Sciences Végétales, BP 42617, 31326 Castanet-Tolosan, France

[(e)] CNRS, UMR5546, BP 42617, Castanet-Tolosan, France

[1] Current address: School of Biological Sciences, Wivenhoe Park, University of Essex, Colchester, CO4 3SQ, United Kingdom

[2] Current address : Agrocampus Ouest, Centre d'Angers, Institut National d'Horticulture et de Paysage, 2 rue André Le Nôtre, 49045 Angers cedex 01, France

* Corresponding author. Tel.: +33 247 36 72 13; fax: +33 247 27 66 60.

E-mail address: marc.clastre@univ-tours.fr

Abstract

Madagascar periwinkle (*Catharanthus roseus* [L.] G. Don, Apocynaceae) produces monoterpene indole alkaloids (MIAs), secondary metabolites of high interest due to their therapeutic value. A key step in the biosynthesis is the generation of geraniol from geranyl diphosphate (GPP) in the monoterpenoid branch of the MIA pathway. Here we report on the cloning and functional characterization of *C. roseus* geraniol synthase (CrGES). The full-length CrGES was over-expressed in *Escherichia coli* and the purified recombinant protein catalyzed the conversion of GPP into geraniol with a Km value of 58.5 µM for GPP. *In vivo* CrGES activity was evaluated by heterologous expression in a *Saccharomyces cerevisiae* strain mutated in the farnesyl diphosphate synthase gene. Analysis of culture extracts by gas chromatography-mass spectrometry confirmed the excretion of geraniol into the growth medium. Transient transformation of *C. roseus* cells with a Yellow Fluorescent Protein-fusion construct revealed that CrGES is localized in plastid stroma and stromules. In aerial plant organs, RNA *in situ* hybridization showed specific labelling of *CrGES* transcripts in the internal phloem associated parenchyma as observed for other characterized genes involved in the early steps of MIA biosynthesis. Finally, when cultures of *Catharanthus* cells were treated with the alkaloid-inducing hormone methyl jasmonate, an increase in *CrGES* transcript levels was observed. This observation coupled with the tissue-specific expression and the subcellular compartmentalization support the idea that CrGES initiates the monoterpenoid branch of the MIA biosynthetic pathway.

1. Introduction

Madagascar periwinkle (*Catharanthus roseus* [L.] G. Don, Apocynaceae) is a pantropical medicinal plant which synthesizes a wide range of complex secondary metabolites known as monoterpene indole alkaloids (MIAs). Several of them are valuable therapeutic compounds, including monomers such as ajmalicine and serpentine used in the treatment of circulatory diseases and anxiety, and heterodimers such as vinblastine and vincristine known as powerful anticancer drugs (van der Heijden et al., 2004). Due to the pharmacological importance of these compounds, the MIA metabolic pathway has been highly studied in the whole plant and in cell suspension culture systems (Zhou et al., 2011). MIAs originate from two convergent pathways. Tryptamine (provided by the indole pathway through decarboxylation of L-tryptophan) and secologanin (provided by the monoterpenoid pathway also known as the iridoid pathway) are condensed into strictosidine, the precursor of all other MIAs (van der Heijden et al., 2004) (Supplementary Fig. S1).

Studies of fluxes in the pathways leading to the formation of MIAs by precursor feeding highlighted that the monoterpenoid branch is limiting for the biosynthesis of alkaloids in cell and tissue cultures of *C. roseus* (Oudin et al., 2007a). A key step in the formation of MIAs is the biosynthesis of the monoterpenoid geraniol from geranyl diphosphate (GPP).

Geraniol feeding of *C. roseus* cell (Lee-Parsons and Royce, 2006) and hairy root cultures (Morgan and Shanks, 2000) resulted in an increase in the formation of the MIAs ajmalicine and tabersonine, respectively, suggesting that the formation of geraniol is a critical step in MIA biosynthesis. To date, periwinkle geraniol synthase (GES) has not been characterized at the molecular level. The present work focuses on the cloning and functional characterisation of *C. roseus* GES, the study of the corresponding gene expression in response to methyl jasmonate, the *in situ* localization of *GES* mRNA and the subcellular localization of the enzyme.

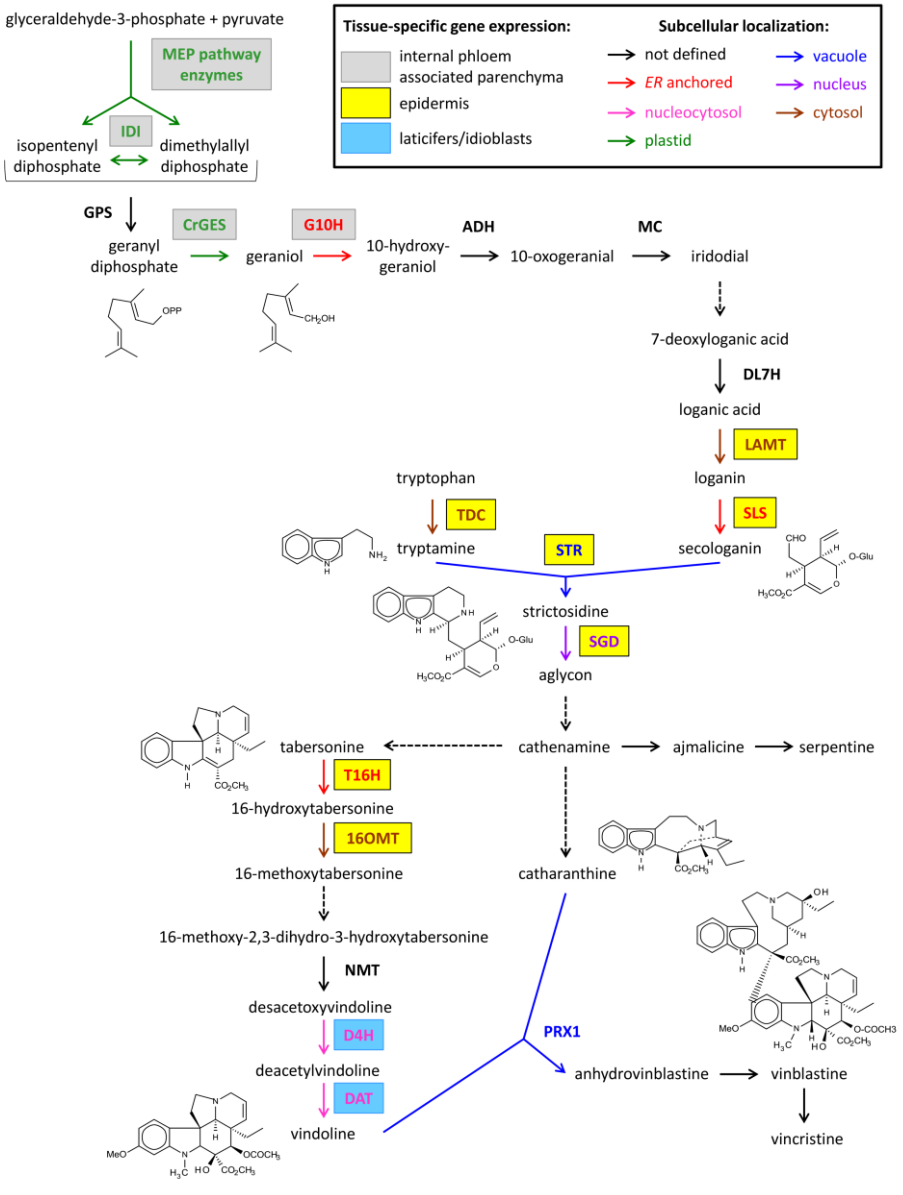

Supplementary Fig. S1. Tissue-specific gene expression and subcellular localization of the enzymes of the monoterpenoid indole alkaloid pathway of *C. roseus*. Broken arrows represent uncharacterized reactions. The localization of CrGES was determined in the present study. 16OMT: 16-hydroxytabersonine-16-*O*-methyltransferase; ADH: acyclic monoterpene primary alcohol dehydrogenase; CrGES: geraniol synthase; D4H: deacetoxyvindoline-4-hydroxylase; DAT: deacetylvindoline 4-*O*-acetyltransferase; DL7H: 7-deoxyloganin 7-hydroxylase; G10H: geraniol 10-hydroxylase; GPS: geranyl diphosphate synthase; IDI: isopentenyl diphosphate isomerase; LAMT: S-adenosyl-L-methionine:loganic acid methyl transferase; MC: monoterpene cyclase; MEP pathway: methyl erythritol 4-phosphate pathway; NMT: 16-methoxy-2,3-dihydro-3-hydroxytabersonine N-methyltransferase; PRX1: peroxidase; SGD: strictosidine β-glucosidase; SLS: secologanin synthase; STR: strictosidine synthase; T16H: tabersonine 16-hydroxylase; TDC: tryptophan decarboxylase. For references see text.

2. Results and discussion

2.1. Isolation of the C. roseus geraniol synthase (CrGES) full-length cDNA

A partial sequence of 554 bp (Genbank ID: EG558318) displaying similarities with known geraniol synthases was identified in a *Catharanthus roseus* EST database. The full-length coding sequence for CrGES (*C. roseus* geraniol synthase) was recovered by 3′ RACE, PhageWalker and GenomeWalker protocols as described in the experimental method section. The *CrGES* sequence has been deposited at NCBI under Genbank ID: JN882024.

The *CrGES* open reading frame of 1770 bp encodes a protein of 589 amino acids in length with a calculated mass of 67.7 kDa. The CrGES protein contains the highly conserved aspartate-rich motif DDxxD (positions 343-347) and the less conserved NSE/DTE motif (positions 485-496) with the consensus sequence (L,V)(V,L,A)-(N,D)D(L,I,V)x(S,T)xxxE (Supplementary Fig. S2). Both motifs are found in several terpene synthases and are involved in the fixation of the diphosphate substrate (Christianson, 2006). Amino acid sequence comparison revealed that CrGES showed similarities with terpene synthases. A high degree of similarity was found with previously characterized geraniol synthases (Supplementary Fig. S2). The highest similarity (64% of identity) was found with the geraniol synthase from *Lippia dulcis* (Genbank ID: GU136162; Yang et al., 2011). Furthermore, CrGES possessed 59% of identity with the *Ocimum basilicum* ortholog (Genbank ID: AY362553, Iijima et al., 2004), 36% with the *Cinnamomum tenuipilum* GES (Genbank ID: AJ457070, Yang et al., 2005) and 33% with the GES from *Perilla frutescens* (Genbank ID: DQ234300, Ito et al., 2007) and *P. citriodora* (Genbank ID: DQ088667, Ito et al., 2007).

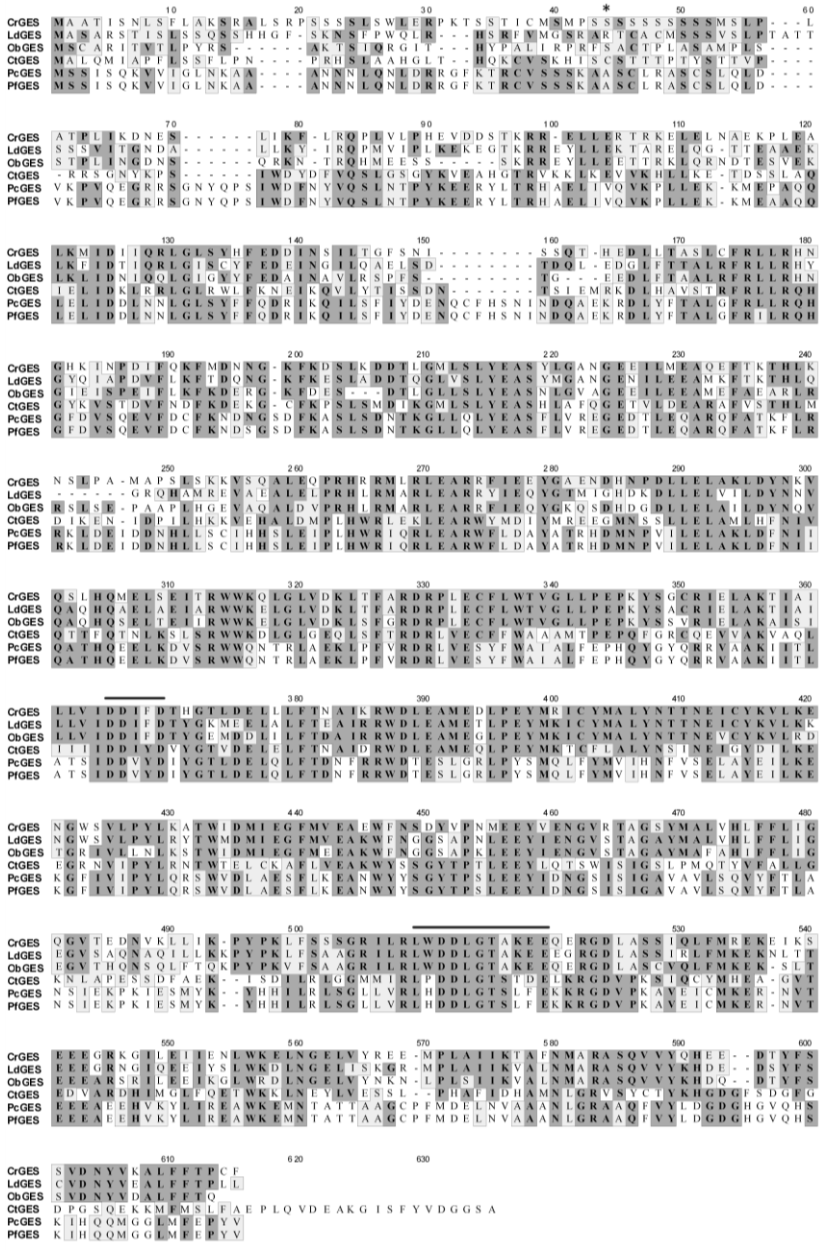

Supplementary Fig. S2. Multiple sequence alignment of plant geraniol synthases. Amino acid comparison of CrGES from *C. roseus* (Genbank ID: JN882024) with geraniol synthases from *Lippia dulcis* (Genbank ID: GU136162), *Ocimum basilicum* (Genbank ID: AY362553), *Cinnamomum tenuipilum* (Genbank ID: AJ457070), *Perilla frutescens* (Genbank ID: DQ234300) and *P. citriodora* (Genbank ID: DQ088667). Identical and similar residues, common to at least three proteins, are shaded in dark and light grey, respectively. The asterisk indicates the position at which the protein was truncated to remove the transit peptide for heterologous expression in yeast. The two upper lines indicate the regions corresponding to the aspartate-rich motif DDxxD and the NSE/DTE motif.

2.2. Functional characterization of the purified recombinant CrGES

The close homology with previously identified geraniol synthases suggested that CrGES catalyzes the conversion of GPP into geraniol. Functional expression was thus carried out to investigate the catalytic activity. The complete *CrGES* open reading frame including the putative N-terminal plastidial targeting peptide flanked by a C-terminal His tag and an N-terminal Strep tag was expressed in *Escherichia coli* and purified by sequential Ni-NTA and Strep-tactin affinity chromatography. Analysis of the recombinant protein by SDS-PAGE and Coomassie Brilliant Blue staining or western blotting and immunoprobing with anti-His antibodies showed the presence of one major band (Fig. 1A). Analysis of reaction products formed after incubation of the protein with GPP showed the presence of a single peak (Fig. 1A), which was identified as geraniol based on the retention time (Fig. 1B) and on the mass spectrum (Fig. 1C and D). A control reaction with boiled protein did not result in detectable products (data not shown). Under the reaction conditions employed, the protein catalyzed the conversion of GPP to geraniol with a K_m value of 58.5 µM for GPP (Supplementary Fig. S3), which is close to the apparent K_m of 55.8 µM reported for GES from the evergreen camphor tree *C. tenuipilum* assayed under similar conditions (Yang et al., 2005).

Fig. 1

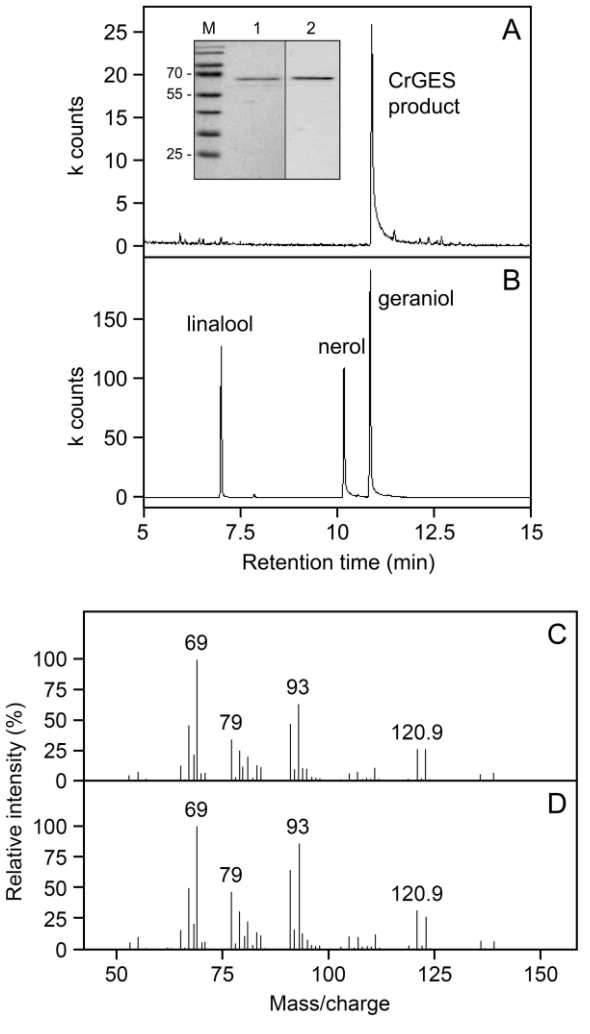

Fig. S3

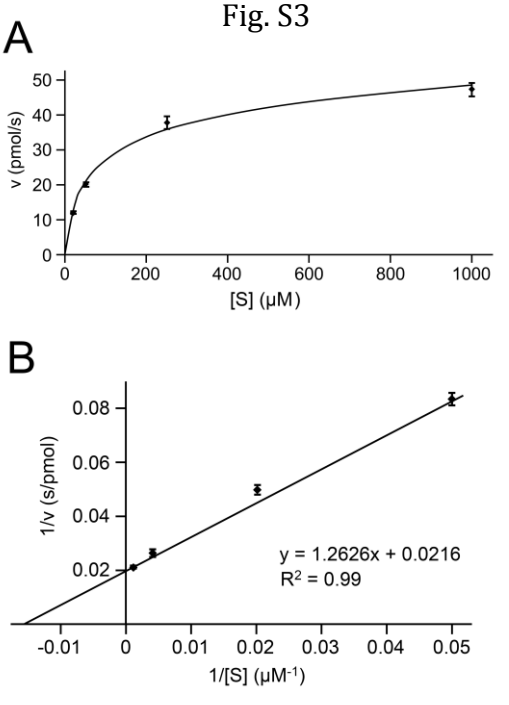

Fig. 1. Analysis of the CrGES-catalyzed reaction product. GC analysis of reaction products with the substrate geranyl diphosphate and recombinant CrGES (A) and of authentic geraniol, nerol and linalool (B). Mass spectra of authentic geraniol (C) and the peak from A (D). The inset in (A) shows the analysis of recombinant CrGES protein. The protein was separated by 10% SDS-PAGE and either stained with Coomassie Brilliant Blue (lane 1) or visualized after western blotting using anti-His antibodies (lane 2). Sizes of relevant marker (M) bands are indicated in kDa.

Supplementary Fig. S3. Michaelis-Menten (A) and Lineweaver-Burk (B) plots of the reaction rate with CrGES and GPP. The data are means ± standard errors of three replicates.

2.3. Expression of CrGES in Saccharomyces cerevisiae FPS mutants

Farnesyl diphosphate synthase (FPS) catalyses the formation of the C_{15} product farnesyl diphosphate (FPP) by two sequential reactions: the initial condensation of isopentenyl diphosphate (IPP) and dimethylallyl diphosphate leading to GPP followed by the condensation of GPP with a second molecule of IPP producing FPP. It is generally accepted that FPS produces only FPP and that no GPP is released from the catalytic site of this enzyme. However, yeast mutant strains containing a mutated FPS, with lower FPS-specific activity, also produced GPP available for the synthesis of geraniol and other related monoterpenes. These compounds originate from GPP and result from endogenous yeast enzymes activities and/or chemical instability of some monoterpenols (Fischer et al., 2011). The over-expression of the heterologous sweet basil (*O. basilicum*) GES in an FPS yeast mutant strain resulted in a marked increase in the production of geraniol (Oswald et al., 2007). Optimisation of the FPS mutation (mutation K197G) coupled to GES expression strongly enhanced (10-20 fold) monoterpene production and led to the excretion of up to 5 mg/l geraniol in the culture medium (Fischer et al., 2011).

We used the yeast strain with the FPS-K197G mutation to evaluate CrGES activity *in vivo*. A truncated coding sequence of *CrGES*, devoid of the plastidial targeting peptide, was cloned into the galactose-inducible expression cassette of the pYES2 vector and introduced into the K197G strain. When transformed with the empty vector, the yeast strain produced a low quantity of various monoterpenes where the major component was geraniol (Table 1). Expression of CrGES greatly increased monoterpenoid production (8.4 fold for geraniol) with the major product geraniol reaching a concentration of approximately 3.3 mg/l in the culture medium. Similar observations were made with the GES from sweet basil, which produced only geraniol when assayed as a recombinant protein *in vitro* (Iijima et al., 2004), whereas expression in the K197G yeast strain resulted in an increase of several monoterpenes with geraniol as the major product (Fischer et al., 2011).

	[Linalool] µg/l	[α-terpineol] µg/l	[Citronellol] µg/l	[Neral] µg/l	[Geranial] µg/l	[Nerol] µg/l	[Geraniol] µg/l
pYES2	104 ± 22	6 ± 3	11 ± 1	ND	ND	9 ± 7	394 ± 27
pYES2+*CrGES*	257 ± 36	18 ± 3	69 ± 14	31 ± 1	54 ± 3	14 ± 3	3.310 ± 221

Table 1. Monoterpene content in the culture medium (µg/l) of a yeast strain with a FPS-K197G mutation transformed with the empty vector pYES2 or with the vector pYES2 containing the *CrGES* coding sequence without the plastidial targeting peptide. Terpenoids were extracted from minimal medium at stationary growth phase. Results are the mean of 5 independent transformants ± standard deviation. ND: Not Detected.

In summary, the results on the heterologous expression of CrGES in yeast mutants are in agreement with the product specificity of the recombinant enzyme and demonstrated that, *in vivo*, CrGES displayed mainly geraniol synthase activity.

2.4. CrGES transcript accumulation

MIA accumulation is induced in *C. roseus* cell cultures growing in a 2,4-D-free medium and can be further increased by the addition of methyl jasmonate (MeJa) (Gantet et al., 1998). This phytohormone stimulates the biosynthesis of alkaloids by inducing the expression of the ESMB genes (encoding enzymes catalyzing Early Steps in Monoterpenoid Biosynthesis) such as those of the methyl erythritol 4-phosphate (MEP) pathway and the geraniol 10-hydroxylase (G10H) gene (Collu et al., 2001; Oudin et al., 2007b) (Supplementary Fig. S1). MeJa also induces the expression of the gene encoding the transcription factor ORCA3 which controls many MIA biosynthetic genes (van der Fits and Memelink, 2000; 2001).

Analysis of transcript levels showed that *CrGES* gene expression was undetectable in untreated cells but strongly induced by MeJa 4 hours post-treatment (Fig. 2). The expression of the *ORCA3* gene, used as a positive control, was strongly increased 30 min post-treatment as previously described (van der Fits and Memelink, 2001). The slower kinetics of gene induction of *CrGES* upon addition of MeJa correlated well with those of *G10H* whose

transcripts also accumulated 4 hours after treatment of periwinkle cell suspensions (Collu et al., 2001).

These results are corroborated by exploiting transcriptomic data from MPGR (http://medicinalplantgenomics.msu.edu/) showing that *CrGES* and *G10H* were both strongly induced by MeJa in hairy roots and young seedlings (Supplementary Fig. S4A). When coupled with the periwinkle metabolome from MPGR, the transcriptomic data revealed that *CrGES* and *G10H* transcript abundance had a similar pattern of distribution in aerial organs (immature leaves, matures leaves and stem, respectively) with those of secologanin and some MIA (Supplementary Fig. S4B). Overall, the comparison of the expression values of *CrGES* and *G10H* within the 22 available periwinkle samples from MPGR revealed that both genes had a very similar expression pattern with a very high Pearson Product-Moment Correlation Coefficient (0.977).

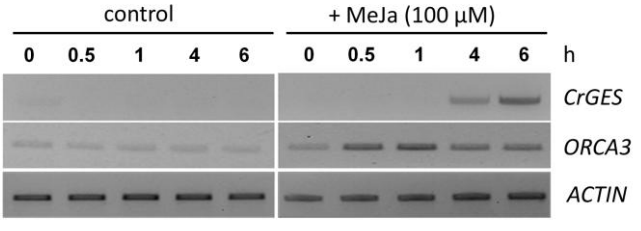

Fig. 2. Time course of *CrGES* mRNA levels in *C. roseus* cell suspension cultures. The cells were not treated or treated with 100 µM MeJa, harvested at the times (h) indicated above the lanes and then analyzed by RT-PCR. The *ACTIN* gene was used as a constitutive control while the *ORCA3* gene was used as a positive control for the MeJa treatment.

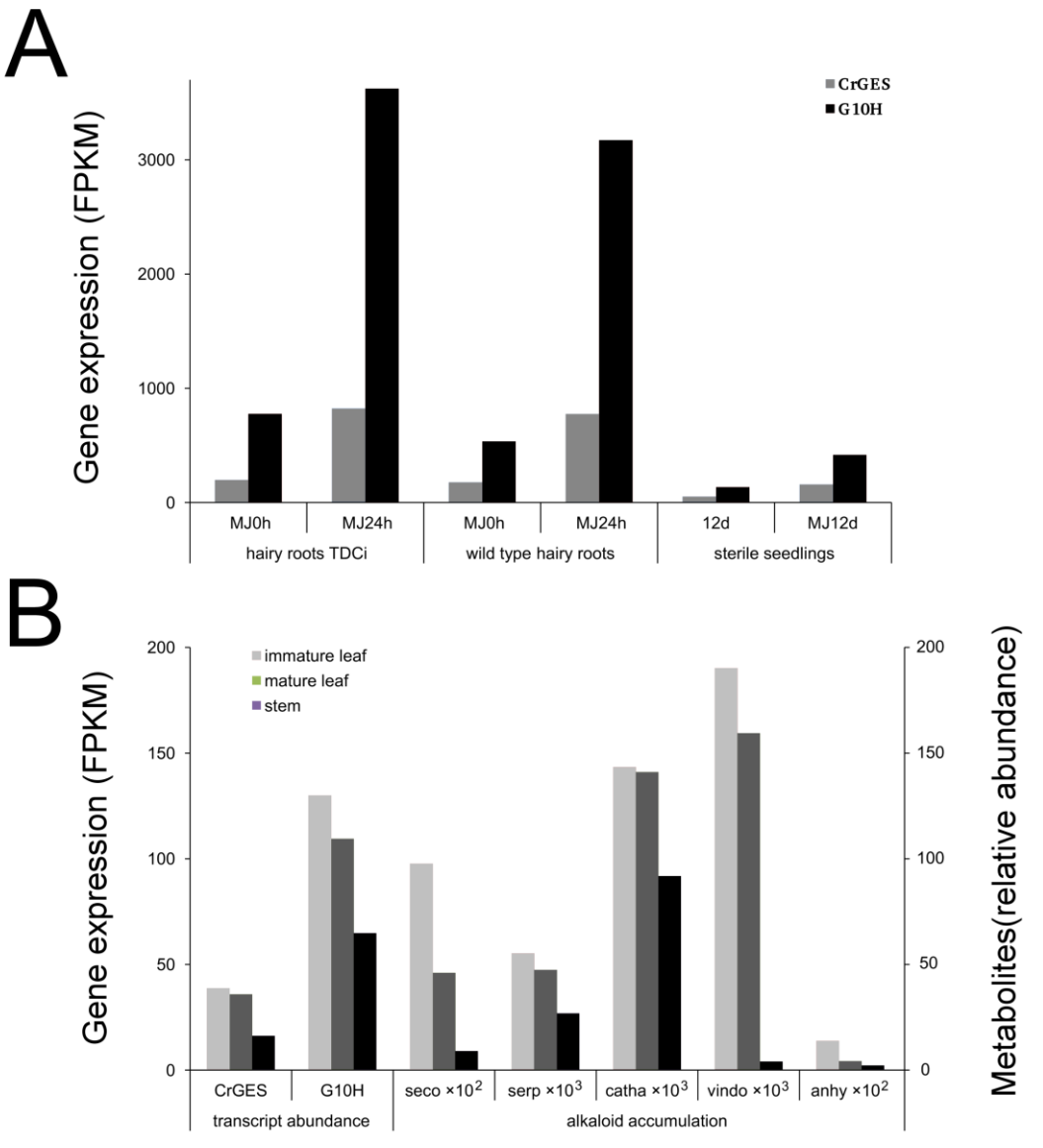

Supplementary Fig. S4. Co-expression of *CrGES* and *G10H* and correlation with alkaloid accumulation. (A) Time course of *CrGES* and *G10H* gene expression (FPKM: fragments per kilobase per transcript per million mapped reads) in two types of hairy roots (TDCi and wild type) and in sterile seedlings treated with MeJa. MJ0h: control at time 0 h; MJ24h: 24 h after 250 μM MeJa treatment; 12d: 12 days old seedlings without MeJa treatment; MJ12d: seedlings treated with 6 μM MeJa for 12 days. (B) Distribution patterns of *CrGES* and *G10H* gene expression (FPKM) and alkaloid relative abundance in aerial organs (immature leaf, mature leaf and stem). Anhy: anhydrovinblastine; catha: catharanthine; seco: secologanin; serp: serpentine; vindo: vindoline. The data were retrieved from the Medicinal Plant Genomics Resource (MPGR, http://medicinalplantgenomics.msu.edu).

2.5. Subcellular localization of the CrGES protein

It is generally accepted that monoterpene synthases that use GPP as a substrate are localized in plastids (Chen et al., 2011). We used ChloroP and PSORT programs to assign confidence values to the presence of an N-terminal plastid transit peptide (Tp) in CrGES. This Tp was predicted by the ChloroP program to be 43 amino-acids in length. To confirm the predicted plastid localization, we determined the subcellular distribution of CrGES through a biolistic-mediated transient expression approach in *C. roseus* cells according to Guirimand et al. (2009). In transiently transformed *C. roseus* cells, the full-length CrGES-YFP fusion protein displayed a pattern of fluorescence which co-localized perfectly with those of the plastidial marker. Fig 3A-C revealed that the full-length CrGES was imported in the plastid stroma but also in stromules (Supplementary Fig. S5), which are thin envelope-bound extensions of the stroma (Natesan et al., 2005). The CrTpGES-YFP fusion protein (corresponding to the first 43 amino acids of CrGES fused to YFP) was also shown to be targeted to the plastid compartment (Fig. 3E-G). This result indicates that the first 43 amino acids are sufficient to direct efficient plastidial import.

The present work constitutes the first demonstration of the presence of a monoterpene synthase within stromules since previous studies have only reported the localization of this family of enzymes in the plastid stroma (Turner et al., 1999; Nagegowda et al., 2008; Lin et al., 2008). The subcellular localization of CrGES in stroma and stromules is also consistent with our previous work showing that the earlier enzymatic steps leading to the formation of geraniol, including the MEP pathway enzyme hydroxymethylbutenyl 4-diphosphate synthase (Oudin et al., 2007; Guirimand et al., 2009) and a long isoform of isopentenyl diphosphate isomerase (IDI) (Guirimand et al., 2012), have a similar compartmentalization in *C. roseus* (Supplementary Fig. S1). Furthermore, it has been demonstrated that stromules are in close association with the endoplasmic reticulum (ER) suggesting that an exchange of metabolites between the two organelles occurs in *vivo* (Guirimand et al., 2009; Schattat et al., 2011). Such a scenario fits well with the next step of the monoterpenoid branch consisting of the conversion of geraniol into 10-hydroxygeraniol catalyzed by G10H (Collu et al., 2001). This enzyme is a cytochrome P450 anchored to the ER membrane with its catalytic domain

likely exposed to the cytosol and in close vicinity with stromules (Guirimand et al., 2009). Thus, it could be hypothesized that stromules facilitate the export of geraniol into the cytosol and thereby its conversion into 10-hydroxygeraniol by the ER-anchored G10H.

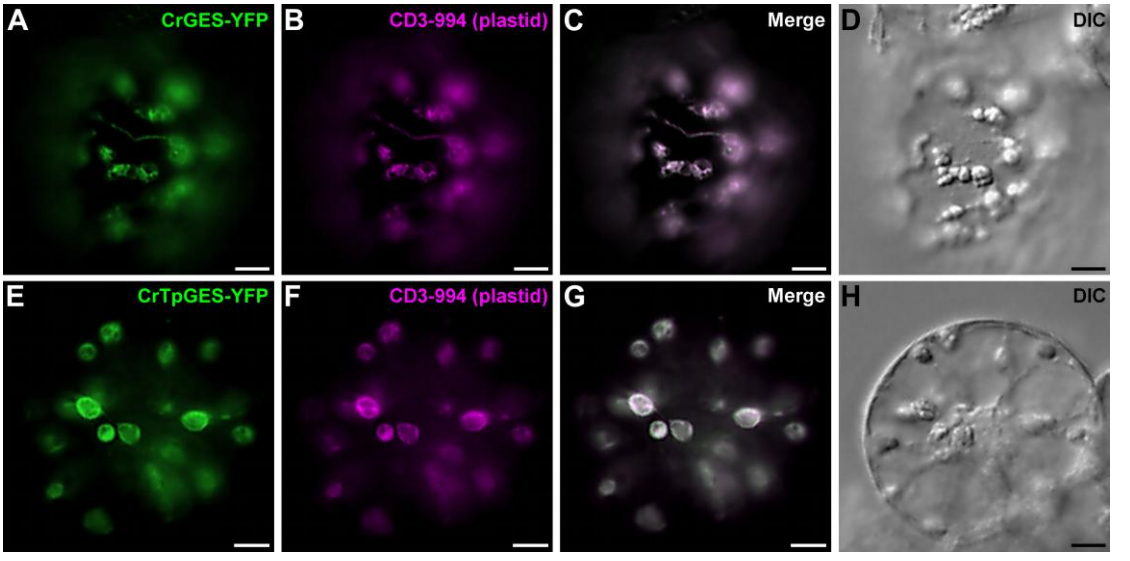

Fig. 3. Subcellular localisation of CrGES. *C. roseus* cells were transiently co-transformed with the plasmid expressing CrGES-YFP (A) or CrTpGES-YFP (E) and the "plastid"-CFP marker CD3-994 (B, F). Co-localization of the two fluorescence signals appeared in white (C, G) when merging the two individual (green/magenta) false colour images. The morphology (D, H) is observed with differential interference contrast (DIC). Bars correspond to 10 µm.

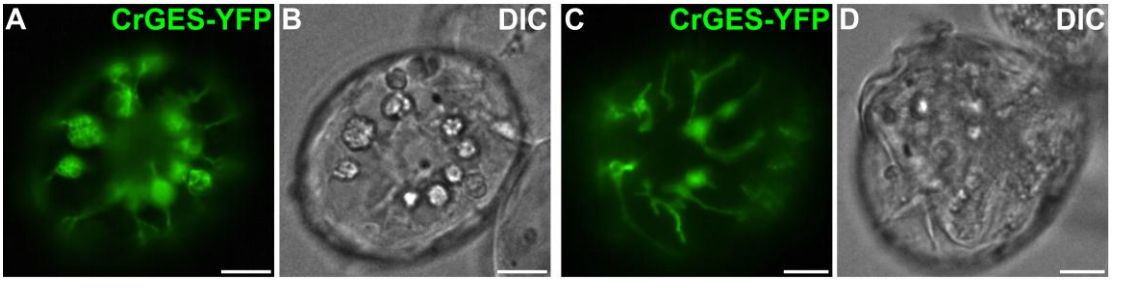

Supplementary Fig. S5. CrGES subcellular compartmentation highlighting localization in stromules. *C. roseus* cells were transiently transformed with the plasmid expressing CrGES-YFP (A, C). The morphology (B, D) is observed with differential interference contrast (DIC). Bars correspond to 10 µm.

2.6. Cell specific gene expression of CrGES

Considerable progress has been made in the past decade in the understanding of the cellular architecture of the MIA biosynthetic pathway revealing its multicellular compartmentalization in aerial organs of *C. roseus* (Supplementary Fig. S1). The late steps, including desacetoxyvindoline-4-hydroxylase and deacetylvindoline-4-O-acetyltransferase, have been localized to laticifers/idioblasts which are specialized alkaloid-accumulating cells (St-Pierre et al., 1999). The intermediate part of the pathway, from the step catalysed by loganic acid *O*-methyltransferase until the step catalyzed by 16-hydroxytabersonine 16-*O*-methyltransferase, occurs in epidermal cells (St-Pierre et al., 1999; Irmler et al., 2000; Burlat et al., 2004; Murata and De Luca, 2005 ; Murata et al., 2008 ; Guirimand et al., 2011a; Guirimand et al., 2011b). The early steps (ESMB, Oudin et al., 2007b), including the MEP pathway, the IDI reaction and the synthesis of 10-hydroxygeraniol by G10H, are present in the internal phloem associated parenchyma (IPAP) cells (Burlat et al., 2004 ; Oudin et al., 2007; Guirimand et al., 2009; Guirimand et al., 2012).

The cellular distribution of *CrGES* transcripts was investigated by RNA *in situ* hybridization performed on young developing leaves. Using the antisense probe, *CrGES* transcripts were specifically detected in the adaxial part of the leaf vascular region (Fig. 4A, B), corresponding to the IPAP cells as confirmed by the co-localization with *G10H* mRNA (Fig. 4E, F; Burlat et al., 2004). No signal was observed with the *CrGES* sense probe, used as a negative control (Fig. 4C, D). This specific labeling of *CrGES* and *G10H* in IPAP cells was also observed in other aerial organs, such as the cotyledons of young seedlings (Supplementary Fig. S6) as well as carpels and stamens (Supplementary Fig. S7). These results clearly indicate that the two consecutive enzymatic steps involving CrGES and G10H occur in IPAP cells.

Fig 4

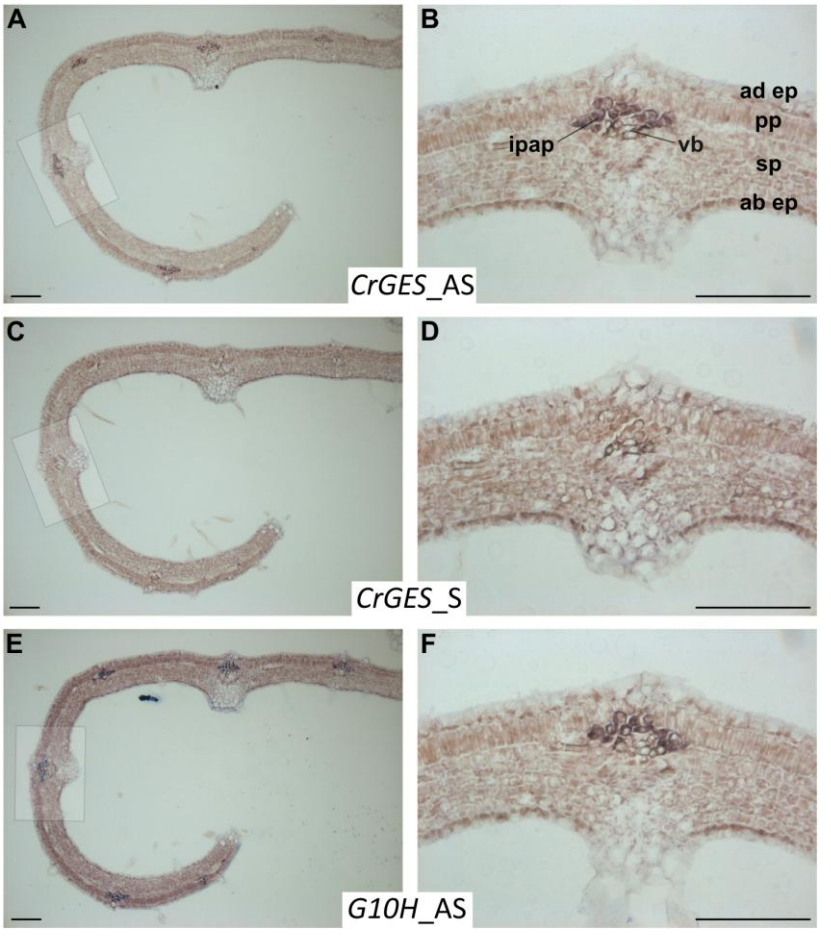

Fig S6

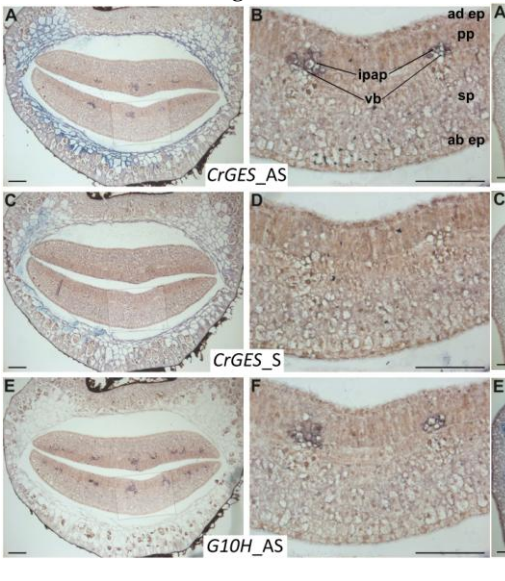

FigS7

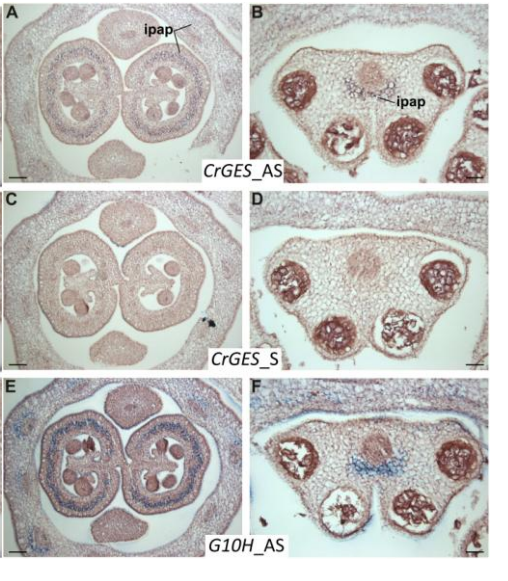

Fig. 4. *In situ* localization of *CrGES* mRNA in young leaves of *C. roseus*. Paraffin-embedded serial longitudinal sections of young leaves were hybridized with digoxigenin-labelled riboprobes, which were subsequently localized with antidigoxigenin-alkaline phosphatase conjugates followed by nitro blue tetrazolium chloride (NBT)/5-bromo 4-chloro-3-indolyl phosphate (BCIP) color development. The antisense probe *CrGES*_AS was used for RNA labeling (A, B) and a control hybridization was performed with the sense probe *CrGES*_S (C, D). Hybridization of the G10H transcripts with the antisense probe *G10H*_AS was used as a positive control (E, F). ab ep: abaxial epidermis; ad ep: adaxial epidermis; ipap: internal parenchyma associated phloem ; pp : palisade parenchyma ; sp : spongy parenchyma ; vb : vascular bundle. Bars correspond to 100 µm.

Supplementary Fig. S6. *In situ* localization of *CrGES* mRNA in cotyledons of young seedlings of *C. roseus*. Paraffin-embedded serial longitudinal sections of emerging cotyledons were hybridized with digoxigenin-labelled riboprobes, which were subsequently localized with antidigoxigenin-alkaline phosphatase conjugates followed by nitro blue tetrazolium chloride (NBT)/5-bromo 4-chloro-3-indolyl phosphate (BCIP) color development. The antisense probe *CrGES*_AS was used for RNA labeling (A, B) and the control hybridization was performed with sense probe *CrGES*_S (C, D). Hybridization of *G10H* transcripts with the antisense probe *G10H*_AS was used as a positive control (E, F). ab ep: abaxial epidermis; ad ep: adaxial epidermis; ipap: internal parenchyma associated phloem ; pp : palisade parenchyma ; sp : spongy parenchyma ; vb : vascular bundle. Bars correspond to 100 µm.

Supplementary Fig. S7. *In situ* localization of *CrGES* mRNA in carpels and stamens of *C. roseus*. Paraffin-embedded serial transversal sections of carpels (A, C, E) and stamens (B, D, F) were hybridized with digoxigenin-labelled riboprobes, which were subsequently localized with antidigoxigenin-alkaline phosphatase conjugates followed by nitro blue tetrazolium chloride (NBT)/5-bromo 4-chloro-3-indolyl phosphate (BCIP) color development. The antisense probe *CrGES*_AS was used for RNA labeling (A, B) and the control hybridization was performed with sense probe *CrGES*_S (C, D). Hybridization of *G10H* transcripts with the antisense probe *G10H*_AS was used as a positive control (E, F). Lines show labeling within the internal parenchyma associated phloem (ipap). Bars correspond to 100 µm.

3. Conclusions

In this report we describe the cloning and functional characterization of the periwinkle cDNA *CrGES* encoding geraniol synthase. The recombinant enzyme produced in *E. coli* catalysed the *in vitro* conversion of GPP into geraniol only. In the yeast FPS mutant K197G expressing CrGES, geraniol was the main enzymatic product formed. The plastidial localization of CrGES suggests that the availability of its product geraniol to the next enzyme G10H could be facilitated through stromule/ER interactions. Furthermore, the induction of *CrGES* expression by MeJa, a phytohormone which stimulates alkaloid accumulation in *C. roseus* cell suspensions, the positive correlation between *CrGES* and *G10H* expression in different tissues of periwinkle and the *in situ* co-localization of *CrGES* mRNA with the ESMB transcripts in IPAP cells of aerial organs support the view that CrGES initiates the monoterpenoid branch of the MIA pathway in *C. roseus*.

4. Experimental

4.1. Plant material and growth conditions

Periwinkle (*Catharanthus roseus* [L.] G. Don, Apocynaceae) cell suspensions (line C20D) were maintained on a 7-day-growth cycle in the B5 medium of Gamborg et al. (1968) supplemented with 58 mM sucrose and 4.5 µM 2,4-dichlorophenoxyacetic acid (2,4-D). For experimental purposes, 7-day-old cells were subcultured in the same medium depleted of 2,4-D. Methyl jasmonate (MeJa) (Sigma-Aldrich, http://www.sigmaaldrich.com) at a final concentration of 100 µM, was added at the fourth day of culture. Accumulation of MIAs is induced in *C. roseus* cells growing in a 2,4-D-free medium and can be further increased by the addition of MeJa (Gantet et al., 1998). Mature *C. roseus* plants, grown in a greenhouse, were used for *in situ* hybridization studies.

4.2. RNA extraction and cDNA synthesis

Frozen cells were ground to a fine powder in liquid nitrogen. Total RNAs were extracted with RNAeasy Plant mini kit (Qiagen, http://www.qiagen.com). The cDNAs were synthesized from 2 µg RNA using the oligo-dT AP primer (Supplementary Table S1) according to the protocol in the Superscript II Reverse Transcriptase kit (Invitrogen, http://www.invitrogen.com) in a final volume of 20 µl.

4.3. Cloning of the CrGES cDNA

Using the BLAST algorithm and the NCBI database, we recovered a *C. roseus* EST (Genbank ID: EG558318) of 554 bp encoding an amino acid sequence which showed similarity with an internal fragment of known geraniol synthases. The EST sequence was used to design primers for the isolation of the 5′ and 3′ ends of the coding sequence of the cDNA.

The 3′-end of the cDNA was recovered by 3′ RACE according to the manufacturer's instructions (Invitrogen). Reverse transcription was performed with the primer AP followed by a first PCR with primers GOS4 and AUAP (from the 3′ RACE kit) and a second nested PCR with primers GOS6 and AUAP (Supplementary Table S1). The resulting PCR fragment was cloned into the vector pGEM-T Easy (Promega, http://www.promega.com) and sequenced.

The 5′-end of the cDNA was recovered by Nested PhageWalker using a *C. roseus* cDNA library (Simkin AJ, unpublished data) constructed with the ZAP Express System (Stratagene, http://www.stratagene.com). The first PCR reaction was carried out with the reverse primer PWGES1 and the forward primer corresponding to the phage plasmid T3 primer (Supplementary Table S1). One µl of this PCR reaction was used for a second PCR reaction with primer T3 and the nested primer PWGES2 (Supplementary Table S1). The resulting amplicon was cloned in pGEM-T Easy and sequenced. The remaining 5′-end 55 bp including the start ATG codon was cloned using the GenomeWalker kit (Clontech, http://www.clontech.com). PCR amplification of genomic DNA extracted from periwinkle leaf was done with primers GWGES4 and AP1 (from the GenomeWalker kit) followed by nested PCR using primers GWGES5 and AP2 (from the GenomeWalker kit) (Supplementary Table S1). This generated a DNA fragment, which was cloned in pGEM-T Easy and sequenced. Following *in-silico* assembly, the full-length open reading frame was identified.

4.4. CrGES expression in Escherichia coli and enzyme purification

The *CrGES* open reading frame was PCR amplified with the primers EcGES1 and EcGES2 (Supplementary Table S1) using a pACTII cDNA library of *C. roseus* MP183L cells treated with yeast extract as template and cloned into pASK-IBA45plus (IBA Biotagnology, http://www.iba-go.com) with BamHI/PstI.

Double Strep/His-tagged CrGES protein was expressed from plasmid pASK-IBA45plus in *Escherichia coli* strain BL21 (DE3) pLysS and purified by sequential Ni-NTA agarose (Qiagen) and Strep-Tactin sepharose (IBA Biotagnology) chromatography. For quality analysis the recombinant protein was run on a 10% (w/v) SDS-PAA gel, transferred to Protran nitrocellulose (Whatman, http://www.whatman.com) by semidry electroblotting,

and the western blot was probed with mouse monoclonal anti-His horseradish peroxidase (HRP) conjugate antibodies (5Prime, http://www.5prime.com). Antibody binding was detected by incubation in 250 µM sodium luminol, 0.1 M Tris-HCl, pH 8.6, 3 mM H_2O_2, 67 µM p-coumaric acid and exposure to X-ray film.

4.5. Enzymatic assays

Enzymatic assays were performed as 1 ml reactions containing 100 mM HEPES-KOH pH 7, 1 mM $MgCl_2$, 100 µM $MnCl_2$, GPP and 4 µg of purified enzyme. For determination of the K_m value reactions contained 20, 50, 250 or 1000 µM GPP. Reaction mixtures were overlaid with 1 ml hexane and incubated at 32 °C for 30 min. For quantitative analysis 5 µg of citronellol was added as an internal standard after incubation. The contents of the tubes were thoroughly mixed by vortexing and kept on ice for 10 min. The tubes were centrifuged at 4000×*g* for 10 min, and the supernatant hexane phase was collected. The extraction was repeated with 1 ml hexane. The pooled hexane phase was dehydrated by passing it through a layer of anhydrous Na_2SO_4 for gas chromatography-mass spectrometry (GC-MS) and GC-flame ionization detector (GC-FID) analysis. Amounts of geraniol formed in enzyme assays were calculated from the resultant GC-FID integral using the relative response factor with respect to the citronellol internal standard. A Lineweaver-Burk plot was constructed to obtain the K_m value.

4.6. GC-MS and GC-FID analysis of the enzymatic product from CrGES expressed in E. coli

For compound identification the CrGES reaction products were subjected to capillary GC-MS, using a Varian Saturn 2000 ion trap mass spectrometer run in electron ionization mode (70 eV). The hexane extract of the reaction mixture was separated on a Varian 3800 gas chromatograph equipped with a DB-5 capillary column (30 m x 0.25 mm, film thickness of 0.25 µm) (Agilent Technologies, http://www.home.agilent.com) using nitrogen as carrier gas at a flow rate of 1.2 ml/min. The separation conditions were: injection split ratio 1:20, injection volume 1 µl , injector temperature 230°C, initial oven temperature 60°C, then linear gradient to 150°C at a rate of 5°C/min followed by a linear gradient to 240°C at a rate of

20°C/min. The transfer line temperature was 275°C, the ion trap temperature 220°C and the manifold temperature 60°C. The mass scan range was 41-500 u with a scan range time of 1 s.

For quantification of geraniol reaction mixtures were subjected to capillary GC-FID. The hexane extract of the reaction mixture was separated on an Agilent 6890 GC equipped with a DB-5 capillary column using nitrogen as carrier gas at a flow rate of 1.2 ml/min. The separation conditions were: splitless mode, injection volume 4 µl, injector temperature 230°C, initial oven temperature 100°C, then linear gradient to 140°C at a rate of 10°C/min followed by a linear gradient to 240°C at a rate of 35°C/min. The detector temperature was 250°C.

4.7. CrGES expression in yeast strains

The 1611 bp partial-length cDNA was amplified with primers GES_F_pYES2 and GES_R_pYES2 (Supplementary Table S1), digested with SacI and BamHI and directionally cloned into the pYES2 expression vector resulting in pYES2-*CrGES*.

Yeast strains were grown aerobically in minimal medium (1.7 g/l Yeast Nitrogen Base (Difco), 5 g/l ammonium sulphate (Merck) supplemented with 1% galactose as carbon source and the required amino acids (His, Leu, Ura) at 50 □g/ml (Euromedex, http://www.euromedex.com). The haploid FPPS mutated strain AE9K197G (*Mat□; his3; leu2Δ0; ura3-; trp1Δ63; YJL167W::kanMX4 [pLB41ERG20K197G]*) (Fischer et al., 2011) was transformed with pYES2 or pYES2-*CrGES* plasmids. Transformed cells were selected for uracil prototrophy on minimal medium supplemented with required amino acids (His, Leu).

4.8. Yeast monoterpene analysis

The cells from a stationary phase culture were harvested by centrifugation (5000×g for 5 min). 3-Octanol (4 µg) and Ethylheptanoate (4 µg) were added as internal standard to 20 ml culture medium supernatant. Monoterpenoids were analysed by Stir Bar Sorptive Extraction and liquid desorption followed by gas chromatography-mass spectrometry method (SBSE-LD-GC-MS) (Coelho *et al.*, 2008) adapted to the laboratory conditions, with 1 µl injection volume. The analyses were performed on an Agilent 6890N gas chromatograph equipped with a Gerstel MultiPurpose Sampler MPS 2 (Gerstel, http://www.gerstel.de)

coupled to an Agilent 5975B inert MSD (Agilent Technologies). The gas chromatograph was fitted with a DB-Wax capillary column (60 m × 0.32 mm i.d. × 0.50 µm film thickness, Agilent Technologies) and helium was used as carrier gas (1 ml/min constant flow). The GC oven temperature was programmed from 45°C to 82°C at 20°C/min then to 235°C at 2.7°C/min (hold 15 min). The injector was set to 230°C and used in pulsed splitless mode (25 psi for 0.50 min). The transfer line, MS ion source and quadrupole analyzer temperatures were maintained at 270°C, 230°C and 150°C, respectively. Electron ionization mass spectra in the range of 29-450 *m/z* were recorded at 70eV. The mass spectra were obtained in full-scan mode and compared with the Wiley 7 MS library and NIST 05 mass spectral databases. Agilent MSD ChemStation software (G1701DA, Rev D.03.00) was used for instrument control and data processing. Total amounts of monoterpenoids were determined using linear calibration curves with an R^2 value of 0.99 over a concentration range from 0 to 6 mg/l.

4.9. In situ hybridization

A CrGES cDNA obtained by PCR amplification with primers GES_Fwd and GES_Rev (Supplementary Table S1) was cloned in pGEM-T Easy and used for the synthesis of sense (SpeI linearization / T7 RNA polymerase) and antisense (SacII linearization / SP6 RNA polymerase) digoxigenin-labelled RNA riboprobes as previously described (Mahroug et al., 2006). For *CrG10H,* a previously described plasmid was used for riboprobe transcription (Burlat et al., 2004). Paraffin-embedded serial longitudinal sections of young developing leaves and of emerging cotyledons and serial transversal sections of carpels and stamens were hybridized with digoxigenin-labelled riboprobes and localized with anti-digoxigenin–alkaline phosphatase conjugates according to Mahroug et al. (2006).

4.10. Generation of constructs for subcellular localisation studies

The full-length *CrGES* cDNA was amplified from *C. roseus* RT-generated cDNA using primers GES_Fyfp and GES_Ryfp (Supplementary Table S1). The full-length *CrGES* cDNA was digested with NheI and cloned into the SpeI site of vector pSCA-cassette YFPi resulting in the plasmid pSCA-*CrGES-YFP*.

A truncated *CrGES* cDNA representing the first 43 amino acids of the transit peptide was amplified using primers GES_Fyfp and reverse primer GES_Ryfp_TP1 (Supplementary Table S1). This amplicon was cloned into the SpeI site of vector pSCA-cassette YFPi resulting in plasmid pSCA-*CrTpGES-YFP*.

4.11. Transient transformation of C. roseus cells and epifluorescence microscopy

Transient transformation of *C. roseus* cells by particle bombardment and YFP imaging were performed following the procedures described by Guirimand et al. (2009, 2010). Briefly, *C. roseus* cells were plated onto solid culture medium and bombarded with DNA-coated gold particles (1 μm) using a 1,100 psi rupture disk at a stopping-screen-to-target distance of 6 cm, using the Bio-Rad PDS1000/He system. Cells were cultivated for 15h to 48h and the protein subcellular localization was determined using an Olympus BX-51 epifluorescence microscope equipped with an Olympus DP-71 digital camera. The "plastid"-CFP (CD3-994) marker (Nelson et al., 2007) obtained from the ABRC (http://www.arabidopsis.org) was used for co-transformation studies with the *CrGES-YFP* and *CrTpGES-YFP* constructs.

4.12. Semi-quantitative RT-PCR

The gene expression levels of *CrGES*, *ORCA3* and *ACTIN* were analysed semi-quantitatively using RT-PCR. The first strand cDNA was synthesized by reverse transcriptase as described above and was used as template for PCR amplification with the primer pairs indicated in Supplementary Table S1. The *ACTIN* gene was chosen as a constitutive external control. The *ORCA3* gene, whose expression is induced by MeJa, was chosen as a positive control for MeJa treatments. PCR reactions were performed with GoTaq polymerase according to the manufacturer's instructions (Promega). Thermocycling conditions were 94°C for 5 min followed by 27 cycles of 94°C for 30 s, 56°C for 30 s and 72°C for 45 s and a final 5 min extension at 72°C. The amplified products were resolved on a 1.5% (w/v) agarose gel and visualized by ethidium bromide staining.

4.13. Sequence analysis

Database searches for similar protein sequences were performed using ***NCBI's BLAST network service*** **(**http://blast.ncbi.nlm.nih.gov/Blast.cgi**).** Protein sequence alignment was performed using ClustalW from the Mac Vector program (MacVector, http://www.macvector.com). The theoretical molecular weight was calculated using the Compute pI/Mw tool (http://expasy.org/tools/pi_tool.html). The chloroplast targeting peptide was predicted using ChloroP (http://www.cbs.dtu.dk/services/ChloroP/) and PSORT (http://wolfpsort.org/) programs.

4.14. Transcriptomic and metabolomic data

The *C. roseus* transcriptome and metabolome are available on the Medicinal Plant Genomics Resource web site (MPGR, http://medicinalplantgenomics.msu.edu). Gene expression levels are provided in the form of FPKM values (Fragments per kilobase per transcript per million mapped reads) for 22 periwinkle samples. The Microsoft Excel PEARSON function calculating the Pearson Product-Moment Correlation Coefficient (PCC) for two sets of expression values (*CrGES* and *G10H*) within the 22 samples was used. The metabolome database provides information about the relative distribution of metabolites (including MIAs) in 19 samples. The relative abundances of individual metabolites were measured on the basis of their molecular mass.

Primer used for reverse transcription	
AP	5′-GGCCACGCGTCGACTAGTACTTTTTTTTTTTTTTTTTT-3′
Primers used for RT-PCR	
GESf	5′-AGAAAATGGAGTTAGAACAGCAGG-3′
GESr	5′-TACACAACTTGGGAAGCTCTTGC-3′
ORCA3f	5′-CCGAGTTCCGAAAGCTGTCAA-3′
ORCA3r	5′-TAGAAGGCTCCGCAGGGAAAC-3′
ACTINf	5′-TGGTGTGATGGTGGGAATGG-3′
ACTINr	5′-TTCCCGTTCTGCTGAGGTTGT-3′
Primers used for 3′RACE	
GOS4	5′-TGAATCTCTCATCAAGTTCTTGCG-3′
GOS6	5′-ATGCAGAAAAACCATTGGAGGC-3′
AUAP	5′-GGCCACGCGTCGACTAGTAC-3′
Primers used for nested phage walker	
PWGES1	5′-ACTGATCTTATGCCCATTGTGTCGAAGC-3′
PWGES2	5′-AGTGAGGAGATCTTCATGAGTTTGGCTGC-3′
T3	5′-AATTAACCCTCACTAAAGGG-3′
Primers used for genome walker	
GWGES4	5′-TCAATGGAGTTGCCAAAGGCAGAGACATGG-3′
GWGES5	5′-AGTCGATGAAGTTTTAGGCCTTTCTAGCC-3′
AP1	5′-GTAATACGACTCACTATAGGGC-3′
AP2	5′-ACTATAGGGCACGCGTGGT-3′
Primers used for CrGES expression in *Escherichia coli*	
EcGES1	5′-CCGGTTGGATCCAATGGCAGCCACAATTAGTAACC–3′
EcGES2	5′-AACCGGCTGCAGTAAAAACAAGGTGTAAAAAACAAAGC-3′
Primers used for CrGES expression in *Saccharomyces cerevisiae*	
GES_F_pYES2	5′-ATAGGGAATATTGAGCTCATGTCTCTGCCTTTGGCAACTCC-3′
GES_R_pYES2	5′-ATAGGGAATATTGGATCCTTAAAAACAAGGTGTAAAAAACAAAGC-3′
Primers used for subcellular localization	
GES_Fyfp	5′-CTGAGAGCTAGCATGGCAGCCACAATTAGTAACC-3
GES_Ryfp	5′-CTGAGAGCTAGCAAACAAGGTGTAAAAAACAAAGCTTTTAC-3′
GES_Ryfp_TP1	5′-CTGAGAGCTAGCTGATGGCATAGACATGCAAATAGTCG-3
Primers used for *in situ* localization	
GES_Fwd	5′-CTGAGAGGATCCTCTCTGCCTTTGGCAACTCC-3′
GES_Rev	5′-CTGAGAGAGCTCTTAAAAACAAGGTGTAAAAAACAAAGC-3′

Supplementary Table S1. Primers used in this study. Restriction sites incorporated for downstream cloning of the amplification fragments are underlined.

Acknowledgements

The research leading to these results has received funding from the European Union Seventh Framework Programme FP7/2007-2013 under grant agreement number 222716 – SMARTCELL. We thank "Le STUDIUM" (Agency for Research and Hosting Foreign associated Researchers in the Centre region, France) for the financial support of Andrew J. Simkin.

References

Burlat, V., Oudin, A., Courtois, M., Rideau, M., St Pierre, B., 2004. Co-expression of three MEP pathway genes and geraniol-10-hydroxylase in internal phloem parenchyma of *Catharanthus roseus* implicates multicellular translocation of intermediates during the biosynthesis of monoterpene indole alkaloids and isoprenoid-derived primary metabolites. Plant J. 38, 131-141.

Chen, F., Tholl, D., Bohlmann, J., Pichersky, E., 2011. The family of terpene synthases in plants: a mid-size family of genes for specialized metabolism that is highly diversified throughout the kingdom. Plant J. 66, 212-229.

Christianson, D.W., 2006. Structural biology and chemistry of the terpenoid cyclases. Chem. Rev. 106, 3412–3442.

Coelho, E., Perestrelo, R., Neng, N.R., Câmara, J.S., Coimbra, M.A., Nogueira, J.M.F., Rocha, S.M., 2008. Optimisation of stir bar sorptive extraction and liquid desorption combined with large volume injection-gas chromatography-quadrupole mass spectrometry for the determination of volatile compounds in wines. Anal. Chim. Acta 624, 79-89.

Collu, G., Unver, N., Peltenburg-Looman, A.M.G., van der Heijden, R., Verpoorte, R., Memelink, J., 2001. Geraniol 10-hydroxylase, a cytochrome P450 enzyme involved in terpenoid indole alkaloid biosynthesis. FEBS Lett. 508, 215-220.

Fischer, M.J.C., Meyer, S., Claudel, P., Bergdoll, M., Karst, F., 2011. Metabolic engineering of monoterpene synthesis in yeast. Biotechnol. Bioeng. 108, 1883-1892.

Gamborg, O.L., Miller, R.A., Ojima, K., 1968. Nutrient requirements of suspension cultures of soybean root cells. Exp. Cell Res. 50, 151-158.

Gantet, P., Imbault, N., Thiersault, M., Doireau, P., 1998. Necessity of a functional octadecanoic pathway for indole alkaloid synthesis by *Catharanthus roseus* cell suspension cultured in an auxin-starved medium. Plant Cell Physiol. 39, 220-225.

Guirimand, G., Burlat, V., Oudin, A., Lanoue, A., St-Pierre, B., Courdavault, V., 2009. Optimization of the transient transformation of *Catharanthus roseus* cells by particle bombardment and its application to the subcellular localization of hydroxymethylbutenyl 4-diphosphate synthase and geraniol 10-hydroxylase. Plant Cell Rep. 28, 1215-1234.

Guirimand, G., Courdavault, V., Lanoue, A., Mahroug, S., Guihur, A., Blanc, N., Giglioli-Guivarc'h, N., St-Pierre, B., Burlat, V., 2010. Strictosidine activation in Apocynaceae: towards a "nuclear time bomb"? BMC Plant Biol. 10, 182.

Guirimand, G., Guihur, A., Ginis, O., Poutrain, P., Héricourt, F., Oudin, A., Lanoue, A., St-Pierre, B., Burlat, V., Courdavault, V., 2011a. The subcellular organization of strictosidine biosynthesis in *Catharanthus roseus* epidermis highlights several trans-tonoplast translocations of intermediate metabolites. FEBS J. 278, 749-763.

Guirimand, G., Guihur, A., Phillips, M.A., Oudin, A., Glévarec, G., Melin, C., Papon, N., Clastre, M., St-Pierre, B., Rodríguez-Concepción, M., Burlat, V., Courdavault, V., 2012. A single gene encodes isopentenyl diphosphate isomerase isoforms targeted to plastids, mitochondria and peroxisomes in *Catharanthus roseus*. Plant Mol. Biol. 79, 443-459.

Guirimand, G., Guihur, A., Poutrain, P., Héricourt,, F., Mahroug, S., St-Pierre, B., Burlat, V., Courdavault, V., 2011b. Spatial organization of the vindoline biosynthetic pathway in *Catharanthus roseus*. J. Plant Physiol. 168, 549-557.

Iijima, Y., Gang, D.R., Fridman, E., Lewinsohn, E., Pichersky, E., 2004. Characterization of geraniol synthase from the peltate glands of sweet basil. Plant Physiol. 134, 370-379.

Irmler. S., Schroder, G., St-Pierre, B., Crouch, N.P., Hotze, M., Schmidt, J., Strack, D., Matern, U., Schroder, J., 2000. Indole alkaloid biosynthesis in *Catharanthus roseus*: new enzyme activities and identification of cytochrome P450 CYP72A1 as secologanin synthase. Plant J. 24, 797-804.

Ito, M., Honda, G., 2007. Geraniol synthases from perilla and their taxonomical significance.

Phytochemistry 68, 446-453.

Lee-Parsons, C.W., Royce, A.J., 2006. Precursor limitation in methyl jasmonate-induced *Catharanthus roseus* cell cultures. Plant Cell Rep. 25, 607-612.

Lin, C., Shen, B., Xu, Z., Kollner, T.G., Degenhardt, J., Dooner, H.K., 2008. Characterisation of the monoterpene synthase gene tps26, the ortholog of a gene induced by insect herbivory in maize. Plant Physiol. 146, 940-951.

Mahroug, S., Courdavault, V., Thiersault, M., St-Pierre, B., Burlat, V., 2006. Epidermis is a pivotal site of at least four secondary metabolic pathways in *Catharanthus roseus* aerial organs. Planta 223, 1191-1200.

Morgan, J.A., Shanks, J.V., 2000. Determination of metabolic rate-limitations by precursor feeding in *Catharanthus roseus* hairy root cultures. J. Biotechnol. 79, 137-145.

Murata, J., De Luca, V., 2005. Localization of tabersonine 16-hydroxylase and 16-OH tabersonine-16-O-methyltransferase to leaf epidermal cells defines them as a major site of precursor biosynthesis in the vindoline pathway in *Catharanthus roseus*. Plant J. 44, 581-594.

Murata, J., Roepke, J., Gordon, H., De Luca, V., 2008. The leaf epidermome of *Catharanthus roseus* reveals its biochemical specialization. Plant Cell 20, 524-542.

Nagegowda, D.A., Gutensohn, M., Wilkerson, C.G., Dudareva, N., 2008. Two nearly identical terpene synthases catalyze the formation of nerolidol and linalool in snapdragon flowers. Plant J. 55, 224-239.

Nelson, B.K., Cai, X., Nebenführ, A., 2007. A multicolored set of *in vivo* organelle markers for co-localization studies in *Arabidopsis* and other plants. Plant J. 51, 1126-1136.

Natesan, S.K., Sullivan, J.A., Gray, J.C., 2005. Stromules: a characteristic cell-specific feature of plastid morphology. J. Exp. Bot. 56, 787-797.

Oswald, M., Fischer, M., Dirninger, N., Karst, F., 2007. Monoterpenoid biosynthesis in *Saccharomyces cerevisiae*. FEMS Yeast Res. 7, 413-421.

Oudin. A., Courtois, M., Rideau, M., Clastre, M., 2007a. The iridoid pathway in *Catharanthus roseus* alkaloid biosynthesis. Phytochem. Rev. 6, 259-276.

Oudin, A., Mahroug, S., Courdavault, V., Hervouet, N., Zelwer, C., Rodriguez-Concepcion, M., St-Pierre, B., Burlat, V., 2007b. Spatial distribution and hormonal regulation of gene

products from methyl erythritol phosphate and monoterpene-secoiridoid pathways in *Catharanthus roseus*. Plant Mol. Biol. 65, 13-30.

Schattat, M., Barton, K., Baudisch, B., Klösgen, R.B., Mathur, J., 2011. Plastid stromule branching coincides with contiguous endoplasmic reticulum dynamics. Plant Physiol. 155, 1667-1677.

St-Pierre, B., Vazquez-Flota, F.A., de Luca, V., 1999. Multicellular compartmentation of *Catharanthus roseus* alkaloid biosynthesis predicts intercellular translocation of a pathway intermediate. Plant Cell 11, 887-900.

Turner, G., Gershenzon, J., Nielson, E.E., Froehlich, J.E., Croteau, R., 1999. Limonene synthase, the enzyme responsible for monoterpene biosynthesis in peppermint, is localized to leucoplasts of oil gland secretory cells . Plant Physiol. 120, 879-886.

van der Fits, L., Memelink, J. 2000. ORCA3, a jasmonate-responsive transcriptional regulator of plant primary and secondary metabolism. Science 289, 295-297.

van der Fits, L., Memelink, J., 2001.The jasmonate-inducible AP2/ERF-domain transcription factor ORCA3 activates gene expression via interaction with a jasmonate-responsive promoter element. Plant J. 25, 43-53.

van der Heijden, R., Jacobs, D.I., Snoeijer, W., Hallard, D., Verpoorte, R., 2004. The *Catharanthus* Alkaloids: Pharmacognosy et Biotechnology. Curr. Med. Chem. 11, 1241-1253.

Yang, T., Li. J., Wang, H.X., Zeng, Y., 2005. A geraniol-synthase gene from *Cinnamomum tenuipilum*. Phytochemistry 66, 285-293.

Yang, T, Stoopen, G., Yalpani, N., Vervoort, J., de Vos, R., Voster, A., Verstappen, F.W., Bouwmeester, H.J., Jongsma, M.A., 2011. Metabolic engineering of geranic acid in maize to achieve fungal resistance is compromised by novel glycosylation patterns. Metab. Eng. 13, 414-425.

Zhou, M.L., Hou, H.L., Zhu, X.M., Shao, J.R., Wu, Y.M., Tang, Y.X., 2011. Molecular regulation of terpenoid indole alkaloids pathway in the medicinal plant, *Catharanthus roseus*. J. Med. Plants Res. 5, 663-676.